Proceedings of the 17th World Congress
The International Federation of Automatic Control
Seoul, Korea, July 6-11, 2008

Variable Speed Control of Wind Turbines: A Robust Backstepping Approach

Selim Sivrioglu * **Ufuk Ozbay** ** **and Erkan Zergeroglu** **

* *Department of Energy System Engineering, Gebze Institute of Technology, Gebze, Kocaeli, 41400 TURKEY (e-mail: s.selim@gyte.edu.tr)*
** *Department of Computer Engineering, Gebze Institute of Technology, Gebze, Kocaeli, 41400 TURKEY (email: ezerger@bilmuh.gyte.edu.tr)*

Abstract: Variable speed wind turbines maximize the energy capture by operating the turbine at the peak of the power coefficient, however parametric uncertainties and disturbances may limit the efficiency of a variable speed turbine. In this study, we present a robust backstepping approach for the variable speed control of wind turbines. Specifically, to overcome the undesirable effects of parametric uncertainties and disturbance effects a nonlinear robust controller have been proposed. The proposed method achieves globally uniformly ultimately bounded rotor speed tracking, despite the parametric uncertainty on both mechanical and electrical subsystems. Extensive simulation studies are presented to illustrate the feasibility and efficiency of the method proposed

1. INTRODUCTION

Wind power generation is a growing sector in the electricity production industry owing to its renewable energy characteristics and reduced environmental problems. Most wind turbines used for power generation are operated at constant speed, however, there is considerable interest in variable speed wind turbines due to their increased energy capture and reduced drive train loads. In variable speed wind turbines, it is possible to control the rotor speed of turbine. This allows the wind turbine system to operate constantly near to its optimum tip-speed ratio. Mainly, it is aimed to follow wind-speed variations in low and moderate velocities to maximize aerodynamic efficiency. Therefore, variable speed wind turbines have potential to maximize energy generation.

The behavior of the variable speed turbine is significantly affected by the control strategy employed in their operationMuldali et al. [1998]. Effectiveness and reliability of the wind power generation is changing depending on the control techniques, that is to make wind power truly cost-effective and reliable for variable speed turbines, advanced control techniques are imperative. To increase the efficiency model based control design approaches can be applied. One drawback however is that mechanical and electrical parameter values of wind turbines are not truly available. Especially in practical applications, uncertainties limit the efficient energy capture of a variable speed turbine. In literature different control strategies have been proposed for variable speed wind turbines Muldali et al. [1998]-Song et al. [2000]. In Muldali et al. [1998], the authors evaluated a variable-speed, stall-regulated strategy which eliminates the need for ancillary aerodynamic control systems. In Boukhezzar and Siguerdidjane [2005] a cascade structure nonlinear controller has been proposed, however the proposed mechanism did not account for the parametric uncertainties of the system. In Song et al. [2000] authors presented two nonlinear controllers, one exact model knowledge and the other adaptive for the rotor velocity tracking however the proposed adaptive controller scheme could only compensate for the uncertainties in the mechanical subsystem and required the exact knowledge of electrical subsystem parameters. In this study, a robust backstepping control that can compensate for the uncertainties of both the mechanical and electrical subsystems is proposed. Compared to the previously introduced nonlinear control methods, the proposed controller can not only compensate for the parametric uncertainty through out the entire system, but also is robust to external disturbances and modelling errors.

The remaining of the paper is organized as follows: In Section II the model of the wind turbine used in this study and the problem statement is given. The error system development and the backstepping controller design scheme is presented in Section III. The stability and boundedness of the closed loop system are investigated in Section IV. While the simulation studies and some concluding remarks are given in Section V and Section VI respectively.

2. SYSTEM MODEL AND PROBLEM STATEMENT

The mathematical model governing the power extraction dynamics of a wind turbine is assumed to be in the following form Song et al. [2000]:

$$J\dot{\omega} + B\omega + K\int_0^t \omega(\tau)\,d\tau + T_d = \frac{P_m}{\omega} - \gamma\frac{P_e}{\omega_e} \qquad (1)$$

where $J = J_m + \gamma^2 J_e$ is the total moment of inertia of the generator-turbine couple, with J_m, J_e being the inertia of the turbine, the inertia of the generator respectively and

γ being the gear ratio. Similarly $B = B_m + \gamma^2 B_e$ is the total friction related, $K = K_m + \gamma K_e$ is the torsion related constant parameters of the turbine and the generator couple and T_d represents uncertain but bounded modelling errors and the disturbance, ω, and $\dot{\omega}$ are the angular velocity of the shaft at turbine end and its time derivative respectively, ω_e is the angular velocity at the generator end, P_m is the wind power, and P_e is the electrical power generated by the system. It is well known that Song et al. [2000], Bergen [1996] the wind power P_m, is related to the angular velocity term and the electrical power generated by the system, P_e, is related excitation current of the generator via the following relationships

$$\begin{aligned} P_m &= k_w \cdot \omega^3 \\ P_e &= \omega_e K_\phi \cdot c\left(I_f\right) \end{aligned} \tag{2}$$

where k_w is a wind speed to power transfer parameter depending on factors like air density, radius of the rotor, the wind speed and the pitch angle, K_ϕ is a machine-related constant, $c(I_f)$ is the flux in the generating system function, and I_f is the field current. Inserting for P_m, P_e from equation (2) back into (1) we obtained generator end angular velocity free model of the system as

$$J\dot{\omega} + B\omega + K\int_0^t \omega\left(\tau\right)d\tau + T_d = k_w\omega^2 - \gamma K_\phi c\left(I_f\right). \tag{3}$$

The exciter (electrical subsystem) dynamics of a wind turbine system is assumed to be governed by

$$L\dot{I}_f + R_f I_f = u_f \tag{4}$$

where L is the constant inductance of the circuit, R_f is the resistance of the rotor field, I_f was defined in (2) and u_f is the field voltage (a synchronous generator). Our control objective is to design the field voltage which ensures that the angular velocity of the shaft at turbine end, ω, would follow a smooth reference trajectory, ω_d , generated according to the operational modes of the turbine, despite the lack of exact knowledge of both the mechanical system parameters of (3) and electrical system parameters of (4). It is also assumed that the generated desired reference trajectory, its integral along time and the first two derivatives are bounded functions (i.e. $\omega_d, \int \omega_d\left(\tau\right)d\tau, \dot{\omega}_d, \ddot{\omega}_d \in \mathcal{L}_\infty$)

3. CONTROL DESIGN

To quantify the control objective, the angular velocity tracking error signal $e\left(t\right)$ is defined in the following form

$$e = \omega_d - \omega. \tag{5}$$

Taking the the time derivative of (5), multiplying both sides of the equation by the total moment of inertia of the generator-turbine couple we obtain

$$J\dot{e} = f + \gamma K_\phi c\left(I_f\right) \tag{6}$$

where (3) was utilized for the $J\dot{\omega}$ term and the auxiliary term $f\left(\dot{\omega}_d, \omega\right)$ contains the mechanical system dynamic parameters and is explicitly defined as

$$f\left(\dot{\omega}_d, \omega\right) = J\dot{\omega}_d + B\omega + K\int_0^t \omega\left(\tau\right)d\tau - k_w\omega^2 + T_d \tag{7}$$

at this point of the analysis we define two more auxiliary terms which will aid our stability analysis, the first one is the so called "desired version" of $f\left(\dot{\omega}_d, \omega\right)$, $f_d\left(\dot{\omega}_d, \omega_d\right)$ that is

$$f_d = f\left(\cdot\right)\big|_{\omega=\omega_d} \tag{8}$$

and the second is the difference between the desired and actual system parameters $\tilde{f}\left(\cdot\right)$ specifically defined as

$$\begin{aligned} \tilde{f} &= f - f_d \\ &= B(\omega - \omega_d) + \int K\left(\omega - \omega_d\right)d\tau - k_\omega\left(\omega^2 - \omega_d^2\right) \end{aligned} \tag{9}$$

Remark 1. Note that the auxiliary terms defined in (7) and (8) can be written as a multiple of a known regression matrix and unknown parameter vector plus the disturbance term as

$$f = W\theta + T_d, \quad f_d = W_d\theta + T_d \tag{10}$$

where the regression matrix $W \in \Re^{1\times 4}$ *contains known and measurable signals, and the desired regression matrix* $W_d \in \Re^{1\times 4}$*, and the unknown parameter vector* $\theta \in \Re^{4\times 1}$ *are defined as*

$$\begin{aligned} W &= \left[\begin{array}{cccc} \dot{\omega}_d & \omega & \int_0^t \omega\left(\tau\right)d\tau & -\omega^2 \end{array}\right] \\ W_d &= \left[\begin{array}{cccc} \dot{\omega}_d & \omega_d & \int_0^t \omega_d\left(\tau\right)d\tau & -\omega_d^2 \end{array}\right] \\ \theta &= \left[\begin{array}{cccc} J & B & K & k_w \end{array}\right]^T \end{aligned} \tag{11}$$

Remark 2. Due to the structure of the auxiliary function f *defined in (7) and the boundedness assumption of the reference signal given in Section 2 we can show that* $\tilde{f}$ *can be upper bounded in the following manner:*

$$\left\|\tilde{f}\right\| \le \rho\left(\|y\|\right) \tag{12}$$

where $\|\cdot\|$ *denotes the standard Euclidean norm,* $y\left(t\right)$ *is the vector function defined as*

$$y = \left[\begin{array}{cc} e & \int e \end{array}\right]^T \tag{13}$$

and $\rho\left(\cdot\right)$ *is a positive definite non-decreasing bounding function*

Adding and subtracting the newly defined auxiliary term, f_d from the right side of (6) we obtain the following open loop dynamics for the error signal

$$J\dot{e} = \tilde{f} + f_d + \gamma K_\phi \cdot c\left(I_f\right) \tag{14}$$

now applying a backsteppingKrstic et al. [1995] argument on (14) we can rearrange the equation to have the following form

$$J\dot{e} = \tilde{f} + f_d + z + \alpha \tag{15}$$

where the $\alpha\left(t\right)$ is an auxiliary control design variable yet to be designed and $z\left(t\right)$ is backstepping variable explicitly defined as

$$z = \gamma K_\phi \cdot c\left(I_f\right) - \alpha. \tag{16}$$

From the open loop error system dynamics the auxiliary control signal $\alpha(t)$ can be designed as

$$\alpha = -k_o e - W_d \hat{\theta} - k_n \rho^2 e - v_{R1} \tag{17}$$

where the desired regression matrix for the mechanical terms, W_d, was defined in *(10)*, $\hat{\theta} \in \Re^{4\times1}$ contains the constant best guest estimates (nominal values) of the unknown parameter vector θ, the bounding function ρ was defined in *(12)*, v_{R1} is an additional robust control term and k_o and k_n are positive constant control gains. The robust term v_{R1} has been introduced to compensate for the mismatch between the actual and estimated parameters and is explicitly defined as follows

$$v_{R1} = \frac{e\left[(\rho_1)_s\right]^2}{\|e\|_m (\rho_1)_m + \epsilon_1} \tag{18}$$

where ϵ_1 is a positive, scalar constant and the positive scalar bounding functions $(\rho_1)_j$ for $j = s, m$ is defined by

$$(\rho_1)_j \geq \left\|W_d\tilde{\theta}\right\|_j + \|T_d\|_j, \quad j = s, m \tag{19}$$

with the notation $\|\cdot\|_j$ for $j = s, m$ being used to define the following functions

$$\|p\|_s = \sqrt{p^T p + \sigma} \quad \|p\|_m = \sqrt{p^T p + \sigma} - \sqrt{\sigma} \quad \forall p \in \Re^n \tag{20}$$

where σ is a small, positive constant.

Remark 3. The backstepping procedure requires that the auxiliary control defined by (17) be differentiable; hence, the robust control terms defined in (18) have been defined with the functions given by (20) to ensure differentiability. In addition, the stability proof requires that the functions defined in (20) be constructed to satisfy the following inequality

$$\|p\|_s \geq \|p\| \geq \|p\|_m \qquad \forall p \in \Re^n. \tag{21}$$

After substituting (17) into (15) we obtain the closed-loop dynamics for $e(t)$ as

$$J\dot{e} = -k_o e + W_d\tilde{\theta} + T_d - v_{R1} + \tilde{f} - k_n\rho^2 e + z \tag{22}$$

where $\tilde{\theta} = \theta - \hat{\theta}$ is the parameter estimation error. The backstepping design procedure also requires the dynamics of the auxiliary term $z(t)$. To this end, we take the time derivative of (16) and multiply by the positive generator inductance term L to obtain

$$L\dot{z} = \gamma K_\phi \frac{\partial c(I_f)}{\partial I_f} L\dot{I}_f - L\dot{\alpha} \tag{23}$$

substituting for $L\dot{I}_f$ and the time derivative of α from (4) and (17) respectively, (23) can be reconstructed to have the following form

$$\begin{aligned} L\dot{z} = \gamma K_\phi \frac{\partial c(I_f)}{\partial I_f}(u_f - R_f I_f) \\ +L\left(\left(k_o + k_n\rho^2\right)\dot{e} + \dot{W}_d\hat{\theta} + \dot{v}_{R1}\right) \end{aligned} \tag{24}$$

inserting for the $\dot{e}$ term form (6) and rearranging the terms we have

$$L\dot{z} = \gamma K_\phi \frac{\partial c(I_f)}{\partial I_f} u_f + Y\phi \tag{25}$$

where $Y(\dot{\omega}_d, \omega, I_f) \in \Re^{1\times7}$ is a regression matrix which contains the known and measurable signals while $\phi \in \Re^{7\times1}$ is the unknown parameter vector containing the combination of both mechanical and electrical uncertain parameters. The explicit definitions of $Y(\dot{\omega}_d, \omega, I_f)$ and ϕ terms are given in *Appendix A*.

From the structure of (25), (22) and the subsequent stability analysis the field voltage u_f is designed in the following form

$$u_f = \frac{1}{\gamma K_\phi \frac{\partial c(I_f)}{\partial I_f}}\left(-k_z z - e - Y\hat{\phi} - v_{R2}\right) \tag{26}$$

where the regression matrix, Y, was defined in *(25)*, $\hat{\phi} \in \Re^{6\times1}$ contains the constant best guest estimates of the unknown parameter vector ϕ, v_{R2} is an additional robust control term and k_z is a positive constant control gain. The robust term v_{R2} has been introduced to compensate for the mismatch between the actual and estimated parameters and is explicitly defined as follows

$$v_{R2} = \frac{z(\rho_2)^2}{\|z\|\rho_2 + \epsilon_2} \tag{27}$$

where ϵ_2 is a positive, scalar constant and the positive scalar bounding functions ρ_2 defined by

$$\rho_2 \geq \left\|Y\tilde{\phi}\right\|. \tag{28}$$

Substituting (26) into (25), the closed-loop dynamics for the backstepping variable z is obtained to have the following form

$$L\dot{z} = -k_z z + Y\tilde{\phi} - e - v_{R2} \tag{29}$$

where $\tilde{\phi} = \phi - \hat{\phi}$ is the parameter estimation error.

4. ANALYSIS

Forming the closed loop error dynamics for the signals $e(t)$ and $z(t)$, we are now ready to state the following Theorem

Theorem 1. The robust controller given by (26) and the auxiliary control input (17) with the robust terms (18) and (27) guarantees uniformly ultimately boundedness of the angular velocity tracking error signal $e(t)$ in the sense that

$$\|e(t)\| \leq \sqrt{\frac{a}{b}\|x(0)\|^2 \exp(-\beta t) + \frac{2\epsilon}{b\beta}(1 - \exp(-\beta t))} \tag{30}$$

where

$$x = \begin{bmatrix} e^T & z^T \end{bmatrix}^T, \tag{31}$$

$$\begin{aligned} a = \max\{J, L\}, \quad b = \min\{J, L\}, \\ \beta = \frac{2\min\{k_o, k_z\}}{\max\{J, L\}}, \; \epsilon = \epsilon_1 + \epsilon_2 + \frac{1}{4k_n}, \end{aligned} \tag{32}$$

$y \in \Re^{2\times1}$ was defined in (13), ϵ_1, ϵ_2, , k_o, k_n, and k_z were defined in (18), (27), (17), and (26), respectively.

Proof 1. We start our proof by defining the following non-negative scalar function

$$V = \frac{1}{2}Je^2 + \frac{1}{2}Lz^2 \tag{33}$$

which can be lower and upper bounded in the following from

$$\frac{1}{2}\min(J,L)\|x\|^2 \le V \le \frac{1}{2}\max(J,L)\|x\|^2 \quad (34)$$

where $x \in \Re^{2\times 1}$ was defined in (31). Taking the time derivative of (33) along (22) and (29) and cancelling common terms, we obtain

$$\begin{aligned}\dot{V} = & -k_o e^2 - k_z z^2 + \left[\tilde{f} - k_n \rho^2 e\right] e \\ & + \left[W_d\tilde{\theta} + T_d - \frac{e\left[(\rho_1)_s\right]^2}{\|e\|_m (\rho_1)_m + \epsilon_1}\right] e \\ & + \left[Y\widetilde{\phi} - \frac{z(\rho_2)^2}{\|z\|\rho_2 + \epsilon_2}\right] z.\end{aligned} \quad (35)$$

After using (19), (12) and (28) , we can upper bound the right-hand side of (35) as follows

$$\begin{aligned}\dot{V} \le & -\min\{k_o, k_z\}\|x\|^2 \\ & + \left[\rho\|e\| - k_n\rho^2 e^2\right] + \left[\rho_1\|e\| - \frac{e^2[\rho_1]^2}{\|e\|\rho_1 + \epsilon_1}\right] \\ & + \left[\rho_2\|z\| - \frac{z^2(\rho_2)^2}{\|z\|\rho_2 + \epsilon_2}\right]\end{aligned} \quad (36)$$

adding and subtracting $\frac{1}{4k_n}$, and then completing the squares of the first bracketed term of (36), we can further upper bound (36) as

$$\begin{aligned}\dot{V} \le & -\min\{k_o, k_z\}\|x\|^2 + \frac{1}{4k_n} \\ & + \left[\rho_1\|e\| - \frac{e^2[\rho_1]^2}{\|e\|\rho_1 + \epsilon_1}\right] \\ & + \left[\rho_2\|z\| - \frac{z^2(\rho_2)^2}{\|z\|\rho_2 + \epsilon_2}\right].\end{aligned} \quad (37)$$

The bracketed terms of (37) can be manipulated as follows

$$\begin{aligned}\rho_i\|r\| - \frac{\rho_i^2\|r\|^2}{\rho_i\|r\| + \epsilon_i} & = \rho_i\|r\|\left(1 - \frac{\rho_i\|r\|}{\rho_i\|r\| + \epsilon_i}\right) \\ & = \epsilon_i\frac{\rho_i\|r\|}{\rho_i\|r\| + \epsilon_i} \le \epsilon_i,\end{aligned} \quad (38)$$

where $r(t)$ is an arbitrary vector and $i \in \{1,2,\}$. Hence, we can use (38) to place an upper bound on the right-hand side of (37) as shown below

$$\dot{V} \le -\min\{k_o, k_z\}\|x\|^2 + \epsilon \quad (39)$$

where ϵ was defined in (32). From the upper bound on $V(t)$ given in (34), we can further upper bound $\dot{V}(t)$ in (39) as shown below

$$\dot{V} \le -\beta V + \epsilon \quad (40)$$

where β was defined in (32). The differential inequality of (40) can now be solved to yield (Dawson et al. [1995])

$$V(t) \le V(0)\exp(-\beta t) + \frac{\epsilon}{\beta}(1 - \exp(-\beta t)). \quad (41)$$

After applying the bounds of (34) to (41), we obtain the following upper bound for $x(t)$

$$\|x(t)\| \le \sqrt{\frac{a}{b}\|x(0)\|^2\exp(-\beta t) + \frac{2\epsilon}{b\beta}(1 - \exp(-\beta t))} \quad (42)$$

where a, b were defined in (32). Based on (42) and the definition of (31), we can show that the angular velocity tracking error $e(t)$ can be bounded as given by (30) (Dawson et al. [1998]). Due to the boundedness of $e(t)$ and $z(t)$ following standard signal chasing arguments, we can shows that all the signals in the closed loop systems (22) and (29) are bounded

5. SIMULATION RESULTS

To verify the performance of the proposed robust controller, two different sets of simulation studies were performed using same system parameters as in Song et al. [2000]. On the first simulation the reference angular velocity signal $\omega_d(t)$ selected as

$$\omega_d(t) = 2 + \sin(t) \quad (43)$$

and on the second one a more realistic reference rotor velocity signal of the form

$$\omega_d(t) = \begin{cases} 0, & u(k) < u_c, \\ X_m(1 + S1), & u(k) < u_r, \\ X_m, & u(k) < u_F, \\ X_m(1 + S2), & u(k) < u_s, \\ 0, & u(k) > u_s \end{cases} \quad (44)$$

have been applied where

$$\begin{aligned} S1 &= \sin\left(\frac{\pi}{2}\frac{(u(k) - s_1)}{d_1}\right) \\ S2 &= \sin\left(\frac{\pi}{2}\frac{(u(k) - s_2)}{d_2}\right)\end{aligned} \quad (45)$$

with

$$\begin{aligned} s_1 = \frac{u_c + u_r}{2},\ \ d_1 = \frac{u_r - u_c}{2}, \\ s_2 = \frac{u_F + u_r}{2},\ \ d_2 = \frac{u_r - u_F}{2}, \\ u_s = 21.3\ m/\sec, X_m = 4.1rad/\sec, \\ u_c = 4.3m/\sec\, u_r = 7.7m/\sec\, u_F = 17.9m/\sec. \end{aligned} \quad (46)$$

Note that the parameter X_m is specified according to the allowable rotor speed. The system parameters for both simulations are considered as

$$\begin{aligned} R_f = 0.02\Omega,\quad L = 0.001H, \\ J = 24490,\quad B = 52,\ \ K = 52, k_w = 3K_\phi = 1.7 \\ c(I_f) = 1000I_f \end{aligned} \quad (47)$$

and the controller gains are selected as

$$\begin{aligned} k_o = 100,\ \ k_z = 0.1,\ \ k_n = 500 \\ \rho = 275,\ \ \rho_1 = \rho_2 = 200 \\ \varepsilon_1 = \varepsilon_2 = 0.4 \end{aligned} \quad (48)$$

In simulation studies the term , T_d, representing the disturbance and modelling errors is set to

$$T_d = 1000(2 + \sin(t)) \quad (49)$$

and for both simulations the best guess estimates of the system parameters were set to 50% of the actual parameters. The results of the first simulation (with sinusoidal reference trajectory)are shown in Figures 1-3. Figure 1 illustrates the reference and actual rotor velocities during the simulation and Figure 2 presents the angular velocity tracking error while the control effort (field voltage) is presented in Figure 3 . As can be seen from the figures, the robust controller achieves good performance. Figures 4-6 are presented to illustrate the performance of the second simulation. Similar to Simulation #1, the reference and actual rotor velocities are presented in Figure 4 with the velocity tracking error graphed in Figure 5 and Figure 6 gives the applied control input to the system.

6. CONCLUSION

In this paper, we have presented a robust backstepping controller scheme for the variable velocity control of wind turbines. The proposed method achieves globally uniformly ultimately boundedness of the tracking error despite the parametric uncertainty on both mechanical and electrical subsystems. We have also theoretically have shown that modelling errors and external disturbance can also be compensated. Simulation studies have been presented to illustrate the performance and feasibility of the proposed method. However in this form our controller requires the integral of the desired rotor velocity profile to be bounded which practically does not impose any weakness Future work will concentrate on removing this theoretical drawback.

REFERENCES

E. Muldaji, K. Pierce, P. Migliore, "Control Strategy for Variable-Speed, Stall-Regulated Wind Turbines", Proceedings of the American Control Conference, Volume 3, pp:1710 - 1714 June (1998)

K. E. Johnson, Y.P.Lucy, M.J. Balas, L.J. Fingersh, "Control of Variable Speed Wind Turbines", IEEE Control System Magazine, Vol. 26, No. 3, pp: 70-81, (2006).

B. Boukhezzar, H. Siguerdidjane, "Nonlinear Control of Wind Turbines for Power Regulation", Proc. of the IEEE Conference on Control Applications, pp: 114-119, Toronto, Canada, (2005).

Y. D. Song, B. Dhinarakaran, X. Y. Bao, "Variable Speed Control of Wind Turbines using Nonlinear and Adaptive Algorithms", *Journal of Wind Engineering and Industrial Aerodynamics*, Vol. 85, pp:293-308, (2000).

A. R. Bergen, *Power System Analysis*, Englewood Cliffs, NJ: Printecive-Hall, (1996).

M. Krstic, I. Kanellakopoulos, P. Kokotovic, *Nonlinear and Adaptive Control Design*, NewYork: John Wiley and Sons, Inc., (1995).

Z.Qu, *Robust Control of Nonlinear Uncertain Systems*, NewYork : Springer-Verlag, (1992).

J.J. Slotine and W. Li, *Applied Nonlinear Control*, Englewood Cliff, NJ: Prentice Hall, (1991).

D.M. Dawson, M.M. Bridges, and Z. Qu, *Nonlinear Control of Robotic Manipulators for Environmental Waste and Restoration*, Englewood Cliffs, NJ: Prentice Hall, (1995).

D.M. Dawson, J. Hu, and T.C. Burg, *Nonlinear Control of Electric Machinery*, New York, NY: Marcel Dekker, (1998).

Appendix A

The regression matrix $Y(\dot{\omega}_d, \omega, I_f) \in \Re^{1\times 7}$ and the unknown parameter vector $\phi \in \Re^{7\times 1}$ of (25) are explicitly defined as follows

$$Y = \Big[-\gamma K_\phi \frac{\partial c(I_f)}{\partial I_f} I_f \;\; \chi\dot{\omega}_d + \dot{W}_d\hat{\theta} + \dot{v}_{R1} \;\; \chi\gamma K_\phi c(I_f) \;\; \chi\omega \;\; \chi\int_0^t \omega(\tau)\, d\tau \;\; -\chi\omega^2 \;\; \chi \Big] \tag{50}$$

$$\phi = \left[R_f \;\; L \;\; \frac{L}{J} \;\; \frac{LB}{J} \;\; \frac{LK}{J} \;\; \frac{Lk_w}{J} \;\; \frac{LT_d}{J} \right]^T \tag{51}$$

where the auxiliary term χ of (50) is

$$\chi = k_o + k_n\rho^2 \tag{52}$$

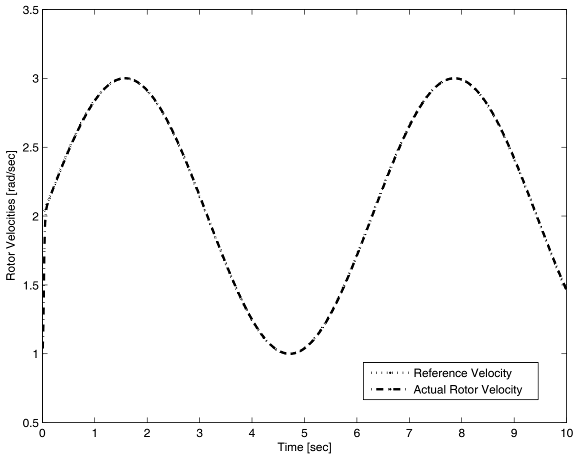

Fig. 1. Reference and Actual Rotor Velocities for Simulation 1

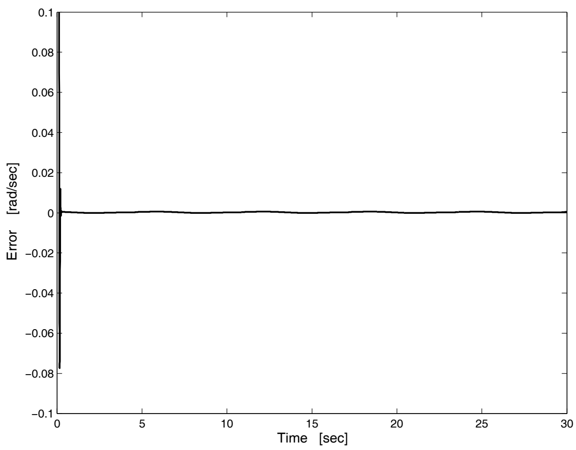

Fig. 2. Angular Tracking Error for Simulation 1

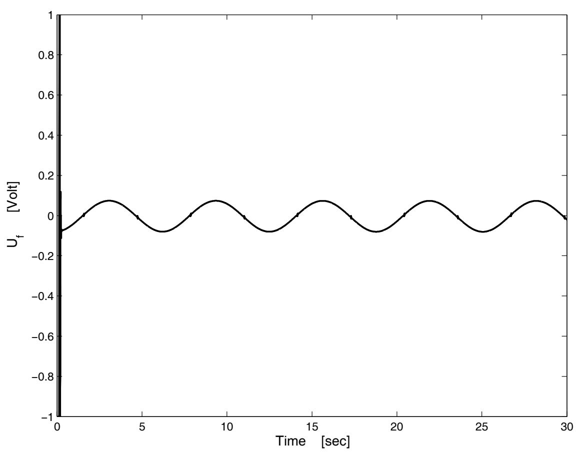

Fig. 3. Control Input (Field Voltage) for Simulation 1

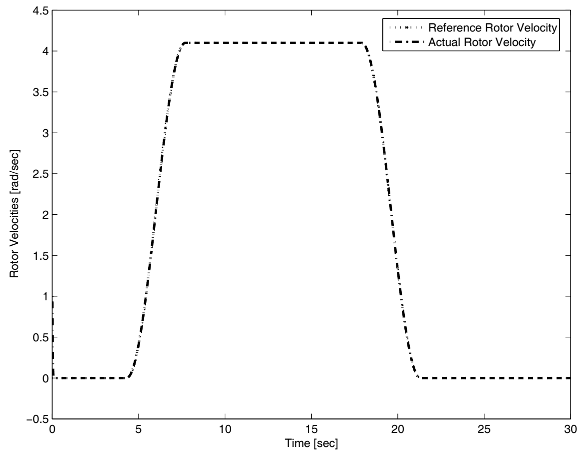

Fig. 4. Desired and Actual Rotor Velocities for Simulation 2

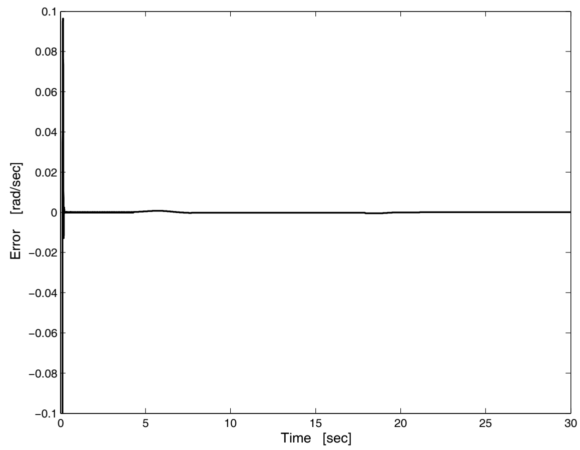

Fig. 5. Angular Velocity Tracking Error for Simulation 2

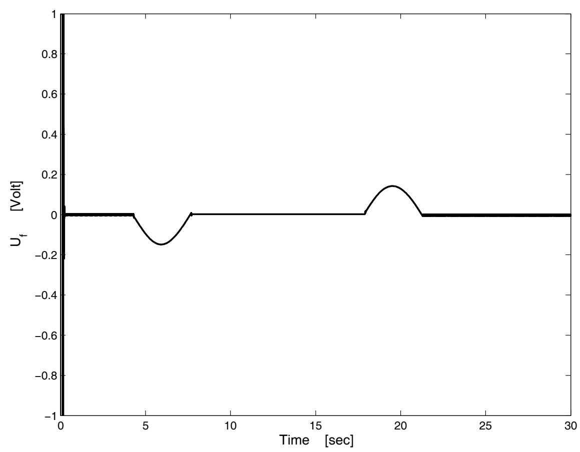

Fig. 6. Control Input (Field Voltage) for Simulation 2